



# IFAR-X: COLLABORATIVE ENGINEERING FRAMEWORK FOR NEXT GENERATION OF AEROSPACE ENGINEERS WORKING ON AIRCRAFT DESIGN

Sparsh Garg<sup>1</sup>, Ana M. P. Silva<sup>2</sup>, Pedro F. Albuquerque<sup>2</sup>, Eric Nguyen Van<sup>3</sup>, Keita Kimura<sup>4</sup>, Yosuke Sugioka<sup>4</sup>, Marcos de R. Jacinto<sup>5</sup>, Prajwal Shiva Prakasha<sup>1</sup> & Björn Nagel<sup>1</sup>

<sup>1</sup>German Aerospace Center (DLR), Institute of System Architectures in Aeronautics, Hamburg, Germany

<sup>2</sup>Centre of Engineering and Product Development (CEiiA), Évora, Portugal

<sup>3</sup>The French Aerospace Lab (Onera), Toulouse, France

<sup>4</sup>Japan Aerospace Exploration Agency (JAXA), Tokyo, Japan

<sup>5</sup>Technische Universität Wien (TU Wien), Vienna, Austria

## Abstract

**At the core of aircraft development lies collaboration, especially crucial for a complex product like an aircraft. The AGILE framework has successfully enabled such collaborative effort, overcoming challenges such as data-driven communication, firewall issues, and tool integration. Extending this collaboration globally, the IFAR-ECN 2023 conference aimed at bringing together leading aerospace engineers from 18 IFAR member countries spanning 4 continents and 9 time zones, to introduce the next generation of engineers to the Collaborative Engineering Framework (CEF). Educating young engineers early in their careers ensures a more seamless and standardized future for collaborative work in aircraft development. This paper presents the framework and guidelines, using three aircraft design use-cases, to demonstrate the collaborative efforts across multiple institutes, establishing a reference aircraft for future IFAR-ECN events. The use-cases are based on three technological advancements: high aspect ratio wing (HAW), composite wing structures and ultra high bypass ratio (UHBR) engines. A design mission is chosen based on a typical short-medium ranged, single aisle, 150 seater Airbus A320 type reference aircraft.**

**Keywords:** Collaborative Engineering; Digital Aircraft Development; Multidisciplinary Design, Analysis and Optimization; System Engineering

## 1. General Introduction

Over the course of the past century, aircraft have transitioned from experimental prototypes to sophisticated, safe, and dependable modes of transportation. This development has shifted from individual trial-and-error efforts in small workshops to a vast collaborative endeavor, involving numerous engineers from various disciplines, working across different organizations and countries, and utilizing digital tools for extensive data-sets. The aircraft industry must continuously innovate to meet the demands for innovative, cost-effective, and high-performance aircraft, often within shorter development timelines. Additionally, the industry must navigate challenges such as global competition, economic fluctuations, security constraints changing certification regulations and reducing non-renewable resources [1, 2, 3].

Enhancing the effectiveness and efficiency of collaboration between disciplinary design experts is viewed as a crucial factor in addressing the aforementioned challenges throughout the aircraft development process. Streamlined collaboration among multidisciplinary specialists is a fundamental requirement for the whole life-cycle of novel aircraft [4, 5]. However, this introduces several non-technical challenges, predominantly identified as the three C's: Complexity, Culture, and Confidence

[6]. Complexity in the design process of a multidisciplinary product like an aircraft arises at multiple levels, encompassing data, personnel, disciplines, and organizations. Additionally, the cross-disciplinary and non-traditional nature of such design tasks can create cultural issues within traditional elements of the process. Consequently, this results in low confidence among traditional aerospace experts regarding novel collaborative multidisciplinary approaches. While traditional technical solutions like email, data and file-sharing software and video-conferencing facilities have been around for decades, they do not entirely mitigate these technical and non-technical barriers. Organizational barriers necessitate legal agreements and contracts to enable engineers to collaborate across organizational boundaries using specific collaboration tools.

A framework of such collaboration enabling tools is setup and demonstrated via the means of the current paper. Thus enabling the required interoperability among diverse tools and data, while adhering to regulations, organizational constraints, and security protocols. The said collaborative engineering framework (CEF) and the involved tools are based on the product development methodology known as the 'AGILE Paradigm' [7]. The AGILE paradigm shifts the focus on accelerating the deployment and the operations of collaborative, large-scale design and optimization frameworks. Its development is in line with the message conveyed during ICAS (International Council of Aeronautical Sciences) 2015 workshop on Complex Systems Integration [8] which emphasised on the need for novel methodologies focusing on encapsulating knowledge and skills in an attempt to manage the increasing aeronautical system design complexities.

Development of a robust collaborative design framework is only the first step in achieving digitization in the world of aerospace. The next challenge at hand is of disseminating the framework to the leading research professionals in the aerospace industry with the intent to potentially establish a standard procedure for collaborative product design, analysis and optimization, in the future. To that end, International Forum for Aviation Research (IFAR) provided a platform to bring together the new generation of experts from 18 different IFAR member countries, spanning across 4 different continents and 9 time zones, shown in Figure 1. It is the aim of the project to educate the next generation of aerospace engineers on the novel collaborative aspect of aircraft design. Therefore, the current paper not only describes the CEF but also emphasises on the need to train young researchers in an attempt to develop a standard method for collaborative aircraft design.



Figure 1 – View of the world map with the IFAR member countries that participated in the ECN event - IFAR-X during June 2023, highlighted in red.

These experts represented their country's leading aerospace research agencies in the IFAR - Early Career Networking (ECN) conference and also the allied event called the IFAR-X Challenge. The participating institutes included Technische Universität Wien (TU Wien - Austria), Na-

tional Research Council (NRC - Canada), Chinese Aeronautical Establishment (CAE - China), Czech Aerospace Research Center (VZLU - Czech Republic), Technical Research Centre of Finland (VTT - Finland), The French Aerospace Lab (ONERA - France), University of Paris-Saclay (UPS - France), German Aerospace Center (DLR - Germany), Budapest University of Technology and Economics (BME - Hungary), Japan Aerospace Exploration Agency (JAXA - Japan), Korea Aerospace Research Institute (KARI - South Korea), Royal Netherlands Aerospace Centre (NLR - Netherlands), Warsaw Institute of Aviation (ILOT - Poland), Centre of Engineering and Product Development (CEiiA - Portugal), National Institute for Aerospace Research "Elie Carafoli" (INCAS - Romania), Agency for Science, Technology and Research (A\* STAR - Singapore), Council for Scientific and Industrial Research (CSIR - South Africa), Linköping University (LiU - Sweden) and National Aeronautics and Space Administration (NASA - USA).

The goal of the challenge is to familiarize the young participants with the CEF developed within DLR and the respective enabler tools involved, followed by the collective application of the newly gathered knowledge to develop a reference high aspect ratio wing (HAW) aircraft using a typical short-medium ranged, single aisle, 150 seater Airbus A320 type aircraft as baseline. The resultant aircraft will serve as a good starting point for future such events and challenges where institutes, disciplinary experts and their respective tools interact and work together to achieve certain sustainable aircraft design objectives. The event took place in Paris, France during the week of the Paris Air Show from 19<sup>th</sup> to 23<sup>rd</sup> June, 2023 with a joint organizational effort from German Aerospace Center (DLR), the French Aerospace Lab (ONERA) and the Institute of Aeronautics and Astronautics of University of Paris-Saclay.

In order to reach the above mentioned objectives, the paper is organized as follows. Section 2 describes the engineering framework, utilized to enable collaboration among the IFAR-X researchers. Details on the MDAO workflow formulated in IFAR-X are provided in section 3. Section 4 collects and discusses the main obtained results in detail. Finally, section 6 addresses the major conclusions of the study.

## **2. Collaborative Engineering Framework**

Collaborative Engineering is simply defined by the authors as a field of engineering where various involved stakeholders work together towards a common goal. Their mutual interests propel them to interact with each other to integrate their expertise in an attempt to derive joint outcomes. By combining the different strengths of multiple disciplines, the collaborative engineering process aims to achieve a more comprehensive and efficient outcome. These disciplines might be provided by heterogeneous teams of specialists distributed among different organizations and across nations. Multidisciplinary Design Analysis and Optimization (MDAO) [9] techniques hold promise in providing key competences in such a paradigm shift. The reason behind adoption of MDAO is to analyse not only the individual disciplines but also the relationships and interaction between them [10]. Thus, the following section takes a closer look into the MDAO part of the chosen AGILE Paradigm, as described by Ciampa and Nagel [7].

### **MDAO Aspect of AGILE Process**

In the AGILE Paradigm, Ciampa et al. [7] lays out a five phase process for establishment and implementation of MDAO systems demanding the solution to a design and optimization problem, see Figure 2. The process starts with defining the design problem in phase one followed by the deployment of the involved design competences phase in two, together forming the upstream part of the paradigm. Phase three is the central phase of the development process which addresses the formalization of the design process resulting in an MDAO workflow which is then integrated and executed in phase four of the process. The process ends with phase five, which deals with the downstream action of decision making. For the sake of the IFAR-X challenge, emphasis is put on the MDAO aspect of the AGILE development process which focuses on the phases 2, 3 and 4 of the paradigm, which are highlighted in Figure 2.

In the Design Competence Deployment phase, the necessary disciplinary competence tools from various partners are identified to address the design and optimization problem. During this step the inputs and outputs for each design competence are specified. The nomenclature and ontologies

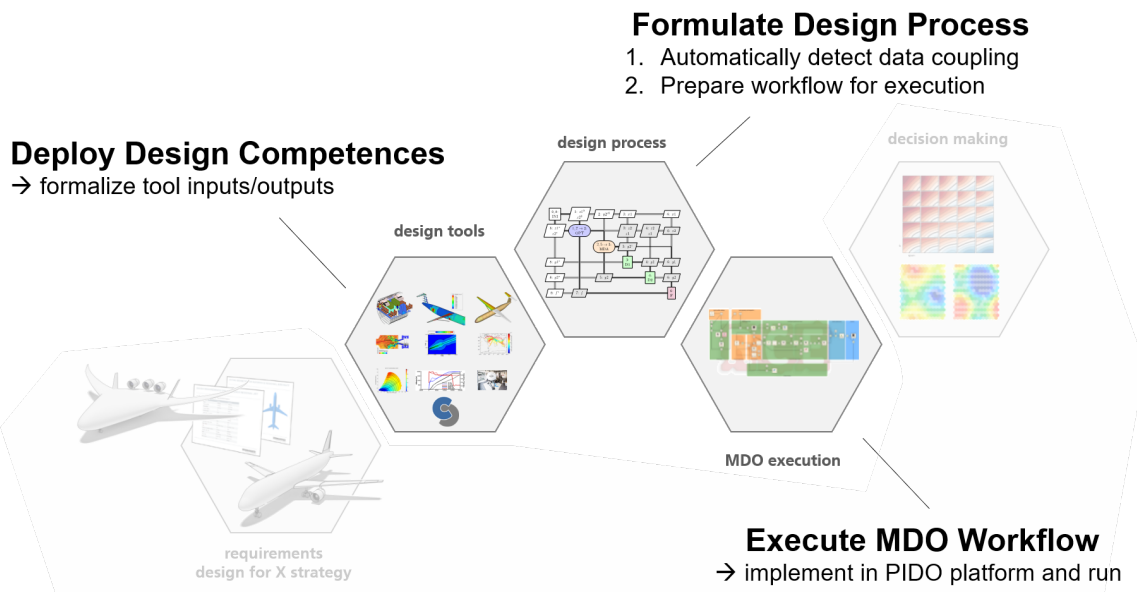


Figure 2 – The AGILE Paradigm for collaborative product development phases with the Phases 2, 3 and 4 highlighted to emphasis on the MDAO aspect of the AGILE paradigm being used in IFAR-X[7]

across different models is also synchronized. To achieve this task, all the competences are interfaced with a common xml based parametric scheme known as the Common Parametric Aircraft Configuration Schema (CPACS)[11]. This is also shown as the first and second step in the CEF shown in Figure 3.

Next phase deals with formulating the design process for the MDAO problem in form of an extended design structure matrix (XDSTM)[12]. It specifies the structure and type of MDAO strategy to be used in the execution phase. Specifications like tool couplings, constraints and driver details for optimizers, convergers and design of experiments (DOEs) are detailed during this step, resulting in an execution plan. To do this, the MDAO Workflow Design Accelerator, MDAX, developed at the Institute of System Architectures in Aviation of DLR, is used (step 3 in Figure 3)[13].

Step 4 of the CEF in Figure 3 corresponds to the Phase four of the AGILE framework in Figure 2. It involves integration of the competences into the Process Integration and Design Optimization (PIDO) platform and execution of the MDAO workflow derived from the previous step. The Remote Component Environment (RCE) [14, 15], is such a PIDO platform which is developed by DLR. Actions like disciplinary model execution, analysis and verification of the results are performed using RCE.

It is important to note that changes can occur in any phase, and they are not necessarily sequential; they are highly iterative. For example, while exploring the design space, a new competence might need to be added to the mix, leading to its integration into the design process, triggering another iteration of the CEF framework. The structured AGILE process architecture aims to enhance flexibility in transitioning between various phases, achieving this through the facilitation of clear visibility and traceability of interactions both within and across these stages. Furthermore, it accelerates the process of formulating and executing collaborative MDAO workflows, as claimed in [7]

### 3. MDAO Workflow for IFAR-X Challenge

The purpose of the project is to enhance collaboration among the next generation of aerospace researchers from different institutes across the world. This is done with an aim of introducing a standardized CEF which can serve as a starting point for establishing a common work approach and mindset for future collaboration. The aim is to further test this approach by designing a reference Airbus A320 type short range, single aisle aircraft. This would serve as a starting point in achieving a more sustainable and fuel efficient reference aircraft configuration which can be used for future detailed studies by the IFAR-X consortium. A typical design mission of 5000 Km range, cruise mach number of 0.78 and flight altitude of 10,500m with a payload capacity of 13.6 tonnes is chosen.

The collaboration is started with a few workshops to familiarize all the disciplinary experts with

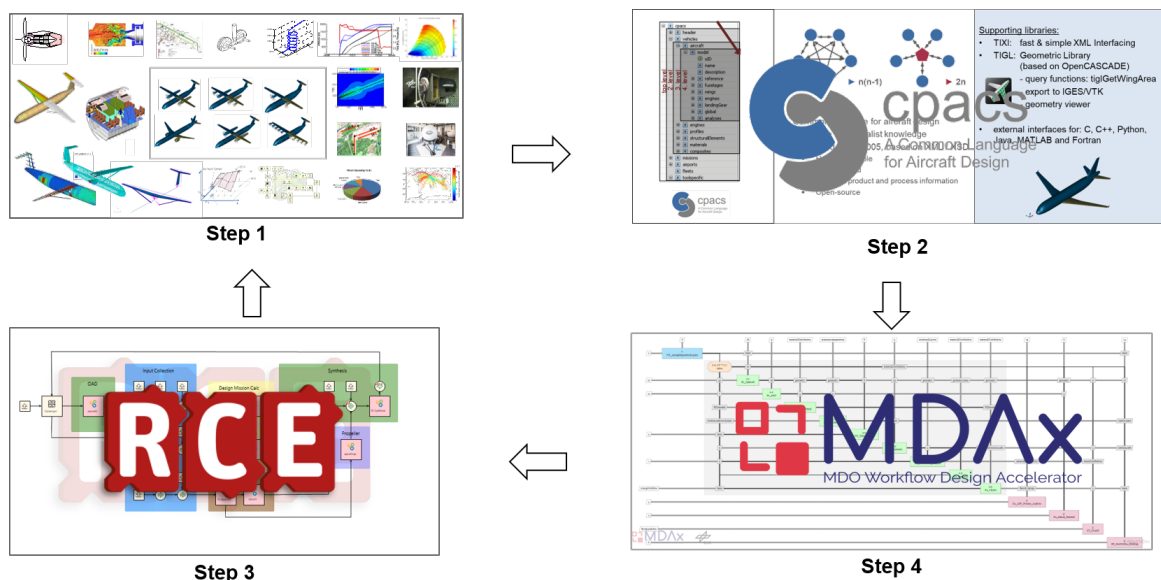


Figure 3 – Collaborative Engineering Framework (clockwise): Step1 - Disciplinary tools are developed at the institutes, providing their expertise, Step2 - CPACS is used as common data schema, Step3 - A framework that enables the execution of loosely-coupled, multidisciplinary workflows, Step4 - Competences are provided as engineering services, shared through RCE.

the methods and tools involved in the CEF like CPACS, MDAX and RCE. Experts from about 18 different countries took part in these workshops. The next step is to understand what competences are brought to the table by each participating institution. This is done via a series of bilateral events. A total of 15 different competences are identified ranging from low and high fidelity aircraft design analysis to airport and air traffic management analysis to cost and life cycle analysis analysis. The next step is to understand the input and output specifications demanded by the each of these competences and also to identify the coupling of each analysis competence with the others in the mix. MDAX is used at this step to add the competences to the MDAO workflow which developed over time to yield the final executable workflow, in terms of an XDSM, as shown in Figure 4. The workflow shows the 15 analysis competences with their respective responsible participant country in a single and possible optimum workflow with minimum feedback and convergence loops. This workflow can now be exported and executed in RCE. Each competence has a dedicated executable tool associated with it which is integrated in RCE. The workflow begins with preliminary overall aircraft design tools which provide a good initial aircraft design based on the top level requirements mentioned earlier in the section. This is followed by a more detailed structural and mass analysis tools while executing a high fidelity aerodynamic analysis tool for wing design. This precedes a convergence loop between the performance analysis tools and the mission simulator tool. Towards the end, tools performing aircraft stability and control calculation, cost calculation, air-traffic management analysis etc. are all executed and can be done so in parallel since there is no coupling between them.

All the competences are then interfaced with CPACS by their respective disciplinary experts by using the variables from the existing aircraft nomenclatures corresponding to their inputs and outputs. If some parameters are missing in the CPACS schema, they are added to the variable tree, leading to an IFAR-X aircraft specific CPACS schema. Next, all the competences are integrated into RCE for the automated execution of the workflow.

A two part study is performed as part of the IFAR-X event that was hosted by ONERA and University of Paris-Saclay in Paris in June 2023 with each part corresponding to a single design loop. To start with the first design loop, the top level requirements of 5000 Km range, cruise mach number of 0.78 and flight altitude of 10,500m with a payload capacity of 13.6 tonnes are taken based on a reference Airbus A320 mission. This yielded the baseline aircraft configuration as shown in Figure 5a. The geometry is generated using TiGL, an open source geometry modeler that is used in the conceptual and preliminary aircraft and helicopter design phase. It creates full three-dimensional

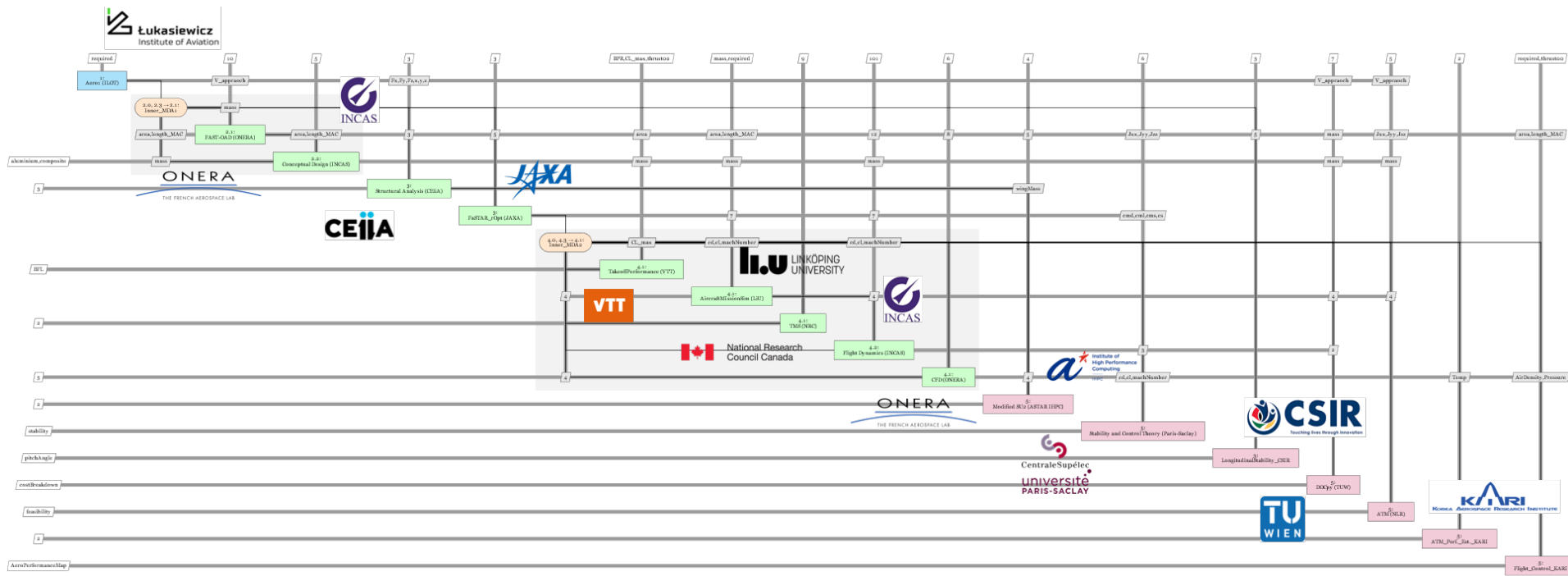


Figure 4 – XDSM for the final MDAO workflow showing all the 15 involved analysis tools and their responsible institutions, used in the IFAR-X event of IFAR-ECN conference and ready to be executed in RCE

models of aircraft from their parametric xml based CPACS description[16]. The resultant geometry has an aspect ratio of 10.27 with a wing span of 35.8m which is consistent with a typical short-medium ranged, single aisle aircraft like the Airbus A320. This part of the study is not only instrumental in yielding a baseline aircraft geometry but also allows the partners to test the framework itself and to address any remaining challenges that are still being faced in terms of adapting to the CEF. In the second design loop, the aspect ratio of the aircraft is increased from 10.27 to 14 and the design mach number is reduced from 0.78 to 0.75 to yield a more fuel efficient aircraft by resulting in a lower requirement of block fuel for the same mission profile. The resultant HAW aircraft has a wing span of 41.8m and a corresponding shorter horizontal stabilizer which can also be seen in the geometric comparison in Figure 5b. The smooth execution of the second iteration reinforced the benefits of the CEF. The design iteration is found to be not only time and resource efficient, but also flexible to any changes in the workflow occurring due to competence additions or modifications.

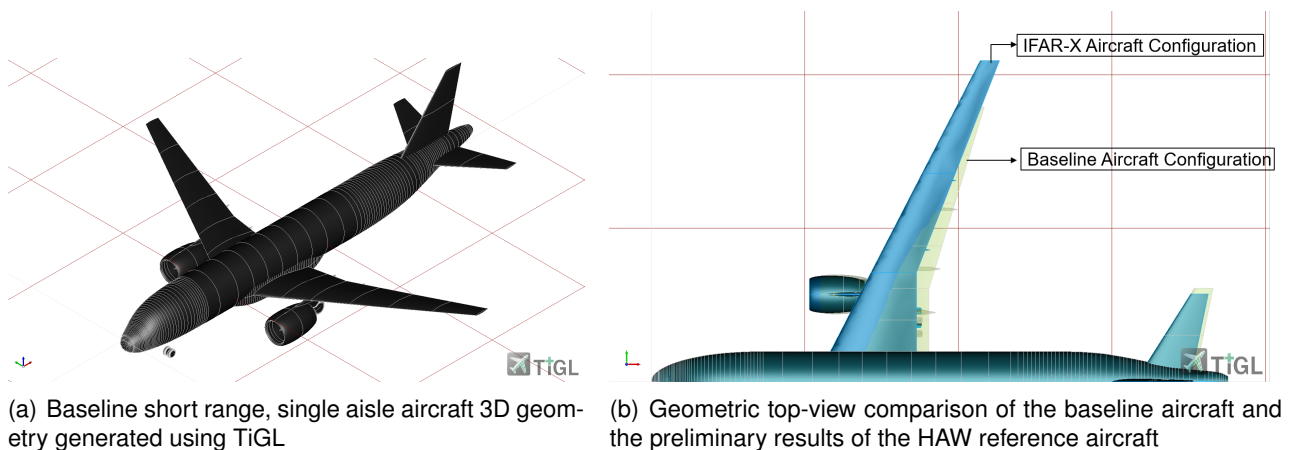


Figure 5 – TiGL generated geometries for the initial baseline aircraft and the post design iteration reference aircraft

#### 4. Use-Case Definition

The framework has been verified and validated as part of the IFAR-X event. The next step is to dive deeper into the detailed design of HAW aircraft by analysing different use cases. The aim is to achieve a more detailed and accurate reference aircraft specifications which can then be used in subsequent aircraft design studies for future IFAR projects.

Three different use-cases (UCs) are identified based on the potential technologies which can influence the baseline A320 like aircraft in becoming more sustainable and thus help in transition to the climate neutral goal of 2050. These technologies are HAW configuration, use of composite for wing structure and using ultra-high bypass ratio (UHBR) engines. Therefore, the primary design variables which are changed from one use-case to the next are aspect ratio, wing structure material and engine by-pass ratio.

The baseline aircraft remains a 150 seater A320 like aircraft with the top level requirements of 5000 Km range, cruise mach number of 0.78 and flight altitude of 10,500m with a payload capacity of 13.6 tonnes. The primary use-case remains the one with transition to a high aspect ratio wing of AR=14. A HAW configuration is proven to have a higher fuel efficiency which results in a lower fuel mass requirement and an overall reduction in negative environmental impact [17]. The Wing Sizer tool of CEiiA is able to deal with composite wing materials, and plays a major role in the second use-case which uses composite material for the wing structure. It should be noted that the configuration of the wing will remain the same as use-case 1 (UC1). The use of composite materials for aircraft structures is becoming more and more common with advancing technology since composite materials make the structure lighter while not compromising on the strength[18]. This provides a major benefit in the aviation industry in terms of lower structure mass, resulting in a better fuel efficiency and performance, which in-turn reflects in lower operating costs[19]. Both, the HAW and composite

material for wing structure, are practical and one of the probable technological advancements which can be seen in the near future to enable transition of current aircraft to future net zero emissions configuration. Another promising technology is the incremental improvement of turbofan engines, especially the transition to current very high by-pass ratio (of the order of 10-11 such as the Leap A1 of the PW1100) to UHBR engines (of the order of 16). It is expected that such UHBR engines can allow up to 10% reduction in Specific Fuel consumption [20]. Finally, both engine and wing structure technology may be used in combination to reach high performance improvement. Therefore, a third use-case, which employs UHBR engines along with HAW configuration aircraft, is also briefly investigated to setup a starting point for future studies. The TLARs for the baseline and the 3 use-cases is listed in the Table 1 which also highlights the the main changes in each use-case.

Table 1 – Top Level Requirements for the baseline aircraft and the three high-aspect ratio wing aircraft use-cases.

Top Level Requirements	Baseline	Use-Case 1: High Aspect Ratio Metallic Wing	Use-Case 2: High Aspect Ratio Composite Wing	Use-Case 3: High Aspect Ratio Metallic Wing with UHBR
Range [Km]	5000	5000	5000	5000
Cruise Mach	0.78	0.78	0.78	0.78
Flight Altitude [Km]	10.5	10.5	10.5	10.5
Payload Capacity [tonnes]	13.6	13.6	13.6	13.6
Aspect Ratio	10.25	14	14	14
Wing Material	Metallic	Metallic	Composite	Metallic
Engine BPR	11	11	11	16

To carry out this analysis, four tools are selected based on their value to the design iteration and their novelty. A brief description of the chosen tools is as follows:

1. **FAST-OAD:** FAST-OAD stands for Future Aircraft Sizing Tool, it is an open source software developed by both ONERA and ISAE-SUPAERO [21]. The software furnishes a framework to easily define a multi-disciplinary analysis and optimisation process. In a multi-disciplinary analysis problem, there usually exists a collection of modules, each providing a single physical analysis, that shares input/output variables through interconnections. The coupled analysis resulting from these interconnections is solved by iterations.

FAST-OAD builds on the OpenMDAO framework to handle the connections between models and brings the ability to exchange one module for another and automatically handle the variable connections. As it is dedicated to aircraft design, it provides a module for simulating the flight mission either with a Breguet integration or with a full 2D time simulation. Semi-empirical models for geometry, aerodynamics, weight and handling qualities are associated with the software to reproduce single aisle aircraft such as the A320 at a preliminary design step.

Within the scope of the IFAR-X challenge, the tool is used to work from Top Level Requirements such as range, payload and cruise Mach number to define a preliminary aircraft geometry. Although, simplified and calculated based on low fidelity models, this initial geometry is the input needed by higher fidelity models and tools. These models are computationally expensive, so it is of interest to analyse only relevant geometries. The preliminary design performed by FAST-OAD ensures that the aircraft geometry and weight satisfy the mission requirements and are worth spending more time and resources to analyse in more details. The higher fidelity analyses then provide refined weight and aerodynamics prediction that can be used for aircraft performance evaluation in an optimization process.

2. **WingSizer:** The WingSizer tool, developed by CEiiA – Portugal in the context of the IFARx 2023, aims to significantly enhance the preliminary structural sizing of wings, and includes



another standalone development, the WinG3N tool, which automatically generates a wing finite element model from its geometric parameters[22].

WinG3N allows its user to define the most relevant design parameters of the wing, including its span, aspect ratio, sweep and dihedral angles, front and rear spar location, stringers and ribs spacings, among others. Once these inputs are defined, the routine creates a Nastran coded bulk data file with the finite element model of the wing, ready to run a linear static or linear buckling analysis, depending on the inputted settings.

WingSizer uses WinG3N to create a baseline wing model which is run using Nastran and post-processed using Altair Hyperview. After running the baseline model, WingSizer will initiate a sizing loop where, for each metallic component, the maximum von Mises stresses are compared with their respective allowable and each component thickness is updated until a positive margin of safety is obtained for all considered failure modes. Likewise, in the case of composite laminate components, the failure index is assessed and if it proves greater than unity, the number of composite layers is increased until the failure index becomes lower than unity. In each loop, the updated model is run using Nastran and post-processed using Altair Hyperview. The tool mainframe is developed in Python and uses an auxiliary TCL script to interact with Altair software and collect the maximum structural stresses, or failure index, for each component under analysis. Globally, not only does it enable a swift preliminary sizing of a given wing configuration, it also unfolds a number of new possibilities in what concerns the early design optimization of an aircraft wing skeleton (internal structure).

Within the collaborative design workflow devised for the current paper, the WingSizer tool performed the preliminary sizing of the wing structure and provided as outputs the thickness distribution per component and the wing structural mass.

3. **FaSTAR:** FaSTAR[23] is a fast unstructured grid based CFD solver developed by JAXA, Japan. It uses orthogonal unstructured lattices generated by HexaGrid. The current compute speed is 1.5 GFlops. For standard aircraft simulations, this translates to 1.8 hours/case. FaSTAR uses the multigrid method and GMRES to achieve high-speed and accurate solutions. The multigrid method is a technique that reduces the resolution of the grid to perform calculations and then expands the solution to a higher resolution grid, thereby reducing computation time. GMRES is an iterative method used to solve large sparse matrices and can provide fast and accurate solutions. It has been validated on the DPW (Drag Prediction Workshop) benchmark problem for accuracy in predicting drag coefficients and is in general agreement with results of other international research organizations.

Within the IFAR-X project, JAXA used FaSTAR to evaluate the aerodynamic performance of the designed aircraft using CFD high-fidelity analysis.

4. **DOCpy:** The direct operating costs tool, DOCpy, was developed by TU Wien, Austria. It provides a simplified model to obtain information about the economic efficiency of a commercial aircraft, giving engineers an overview of expected costs for acquisition and operation of the aircraft, and a way to compare distinct design options during preliminary design.

The input from other tools consists of cruise flight Mach number and altitude, number of passengers, design masses (maximum take-off, operating empty, payload, and fuel), engine mass and engine static thrust. From the data available, an estimate is made for the flight duration and number of flight cycles in a year, and the annual cost breakdown for an aircraft is given, splitting costs into the following categories: capital, crew, maintenance, fuel, payload handling, landing fees and ATC fees. The capital cost includes the total price of the aircraft, and depreciation and interest over time. The crew cost represents the expenses in wages paid to the cockpit and cabin crew. The maintenance cost measures expenses related to in-service maintenance, repairs, and overhauls. Charges from air traffic control are calculated as defined by EUROCONTROL[24]. The landing and payload handling fees are intrinsic to the operational scenario of the aircraft. The model applies methods for the European scenario exclusively.

The four tools discussed above are part of a reduced version of the IFAR-X workflow which can now be employed to carry on detailed studies for different use-cases. The resultant reduced workflow can be seen in Figure 6.

The above mentioned tools and the consequent workflow, deals with a multi fidelity, multi objective MDAO problem. Three primary objectives are identified for the design iterations for the detailed aircraft design phase. These are wing structural weight, block fuel mass and the direct operating cost (DOC). The design process begins with the FAST-OAD tool analysing the preliminary TLARs to determine the geometry and masses (maximum take-off mass, operational empty mass etc.) of the aircraft. These along with the TLARs serves an input to the FaSTAR CFD tool. FaSTAR continues the process by performing the CFD analysis of the wing of the aircraft to generate aerodynamic performance data and the wing loads distribution. It should be noted, that since the chosen use-cases are more centered around changes to the wing, the high fidelity CFD analysis is restricted to the wing geometry rather than the whole aircraft. This restricts the run time of the high fidelity FaSTAR tool to a few hours, thus saving time and resources while still providing an insight into the physics of the chosen configurations. The aerodynamic performance parameters like wing lift and drag polars are then fed-back to FAST-OAD leading to a convergence loop between the two tools. Also, the wing loads output, along with the TLARs and the outputs from FAST-OAD, are crucial for WingSizer tool for its wing sizing operation. WingSizer uses the wing load distribution and takes into account the wing material to size the wing and output a wing weight. This wing weight is fed-back into FAST-OAD. After receiving the aerodynamic data and wing mass as feedbacks, FAST-OAD generates a more accurate estimate of the masses, wing geometry and overall aircraft performance parameters. This loop between the tools from ONERA, JAXA and CEiiA is continued until a converged solution is obtained. For practical purposes, this convergence loop is truncated after only a few iterations to conserve time and resources. Finally, the outputs of these three tools is provided as input to the DOCpy tool from TU Wien. This tool takes into account the mission definition and the masses to estimate the various operating costs. This process is first verified by analysing the design of the baseline aircraft which is based on an A320 like reference aircraft. Based on the accuracy of the results certain analysis factors are modified to obtain a reliable workflow for the analysis of the three use-cases.

Since the purpose of the paper is to demonstrate the prowess of the CEF in designing detailed aircraft configuration more efficiently, therefore, the scope is limited to performing a design of experiment analysis for the various use-cases. Thus, a full optimization study is out of the scope of this paper and can be reserved for future collaborative projects dedicated for aircraft design.

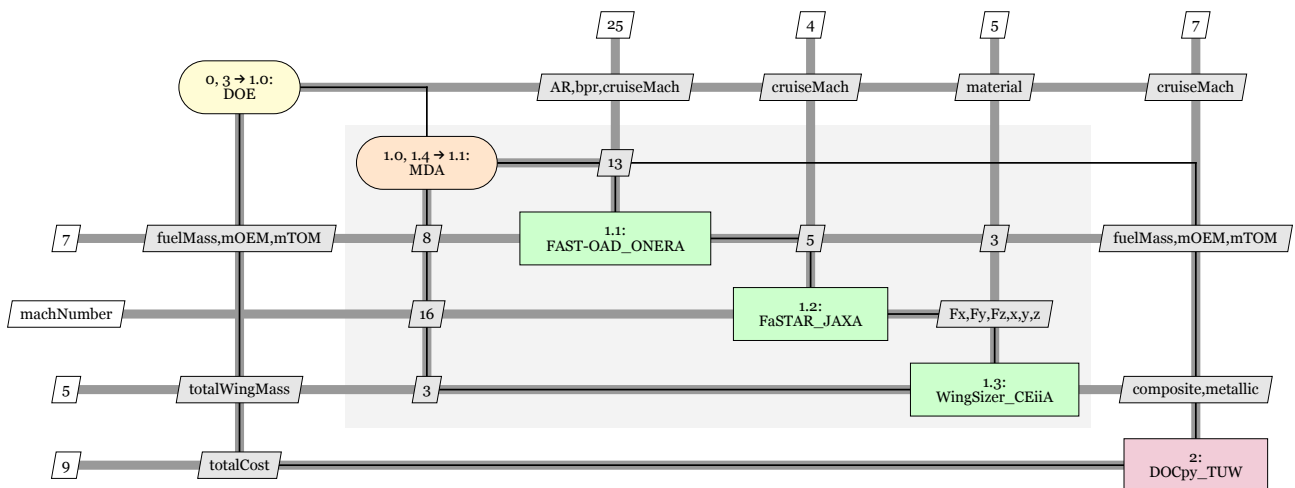


Figure 6 – Reduced version of the XDSM used in IFAR-X event including four primary tool for aircraft design analysis of the 3 use-cases

### 5. Results

This section will present the preliminary results for the baseline aircraft configuration and the 3 use-cases. It is important to reiterate that the goal of the study is not to design novel aircraft

but to demonstrate that the CEF can be used to yield a more efficient design process for the next generation of sustainable aircraft. The workflow and the order of execution of the tools, including convergence loops, has been discussed in the previous section. However, to make the results more comprehensible, this section will start with first discussing the results of the high fidelity aerodynamics analysis, followed by the sizing of the wing. Consequently, a brief insight into the overall aircraft design and integration is presented, followed by a cost analysis to conclude.

### 5.1 High Fidelity Aerodynamic Analysis

To evaluate the aerodynamic performance and load of the aircraft, CFD analysis using FaSTAR has been conducted.

#### *Computational Setup:*

The calculations are performed with RANS (Reynolds-Averaged Navier-Stokes) simulations employing the Spalart-Allmaras noft2-R turbulence model. For simplicity, only the main-wing is modeled for generating computational grids. Since all the three use-cases have HAW wing configuration, the wing geometry only changes from baseline case to the first use-case and remains the same for use-case 2 (UC2) and use-case 3 (UC3). Therefore, a CFD analysis is only performed for baseline case and UC1. The wing geometry is obtained by extracting CAD data from the xml file using TiGL. To reduce computational costs, a half-wing model has been constructed, applying symmetry boundary conditions to the ( $Y = 0$ ) plane. The grids are created based on an unstructured grid, however the wing surface and its surroundings (around the boundary layer) has been constructed as a structured grid. The total number of grid cells is approximately 12 million and 19 million for baseline aircraft wing and HAW UC1 (same as UC2 and UC3), respectively, and the grid spacing of the first layer on the wall is determined so that  $Y_+$  is less than 1. The analysis conditions for FaSTAR are summarized in Table 2 and the grid information is highlighted in Table 3. Figure 7 provides a glimpse of the resultant mesh.

Table 2 – Numerical conditions for FaSTAR

Governing equation	Reynolds-Averaged Navier-Stokes equation
Time integration	LU-SGS
Reconstruction	2nd order MUSCL
Advection terms	HLLEW
Slope limiter	Minmod
Turbulence model	Spalart-Allmaras noft2 Rotation correction (SA-noft2-R)

Table 3 – Computational grid settings

-	<b>Baseline Wing Geometry</b>	<b>High-AR Wing Geometry</b>
Total number of cells	12 millions	19 millions
1st cell size of wall surface	2.0x10e-6 [m]	2.0x10e-6 [m]
Growth rate	1.2	1.2

#### *CFD Results:*

Figure 8 show the pressure distribution and the friction stress distribution in the direction of flight, obtained through CFD analysis. It can be observed that there is a sudden change in the distribution at the mid-chord region across the entire span. This suggests the presence of shock waves on the wings of an aircraft flying in the transonic regime. The pressure distribution shows a rapid pressure recovery, and the friction stress distribution exhibits a sudden decrease. The HAW configuration has lower skin friction coefficients due to a shorter chord and higher thickness to chord ratio, thus leading to a reduction in skin friction drag.

Figure 9 illustrates the primary aerodynamic performance curves. In the HAW configuration, the aspect ratio of the wing is increased as compared to the baseline configuration, reducing the

influence of wingtip vortices across the span. This results in a decrease in induced drag and an increase in lift curve slope. The current results align with these trends, indicating that the design modifications have been appropriately reflected.

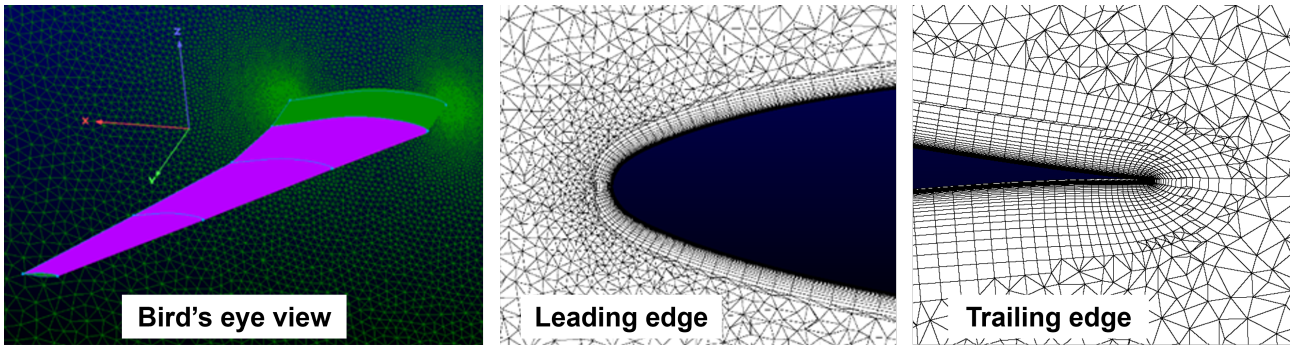


Figure 7 – Overviews for computational grid generated for the wing geometry

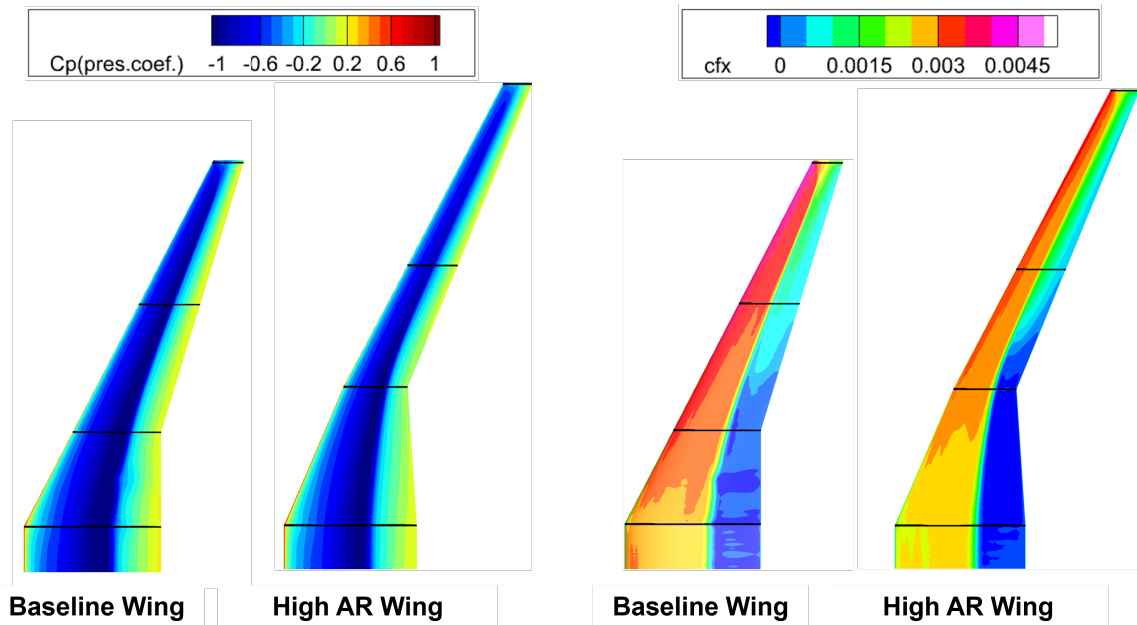


Figure 8 – Wing contours obtained by FaSTAR (left: pressure contours right: friction stress contours)

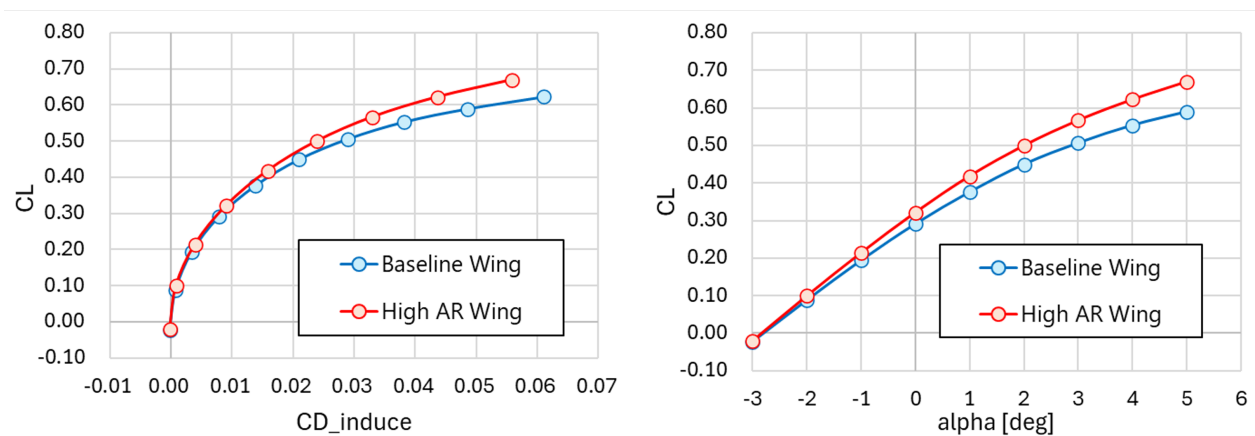


Figure 9 – Aerodynamic performance comparison between the baseline wing and HAW configurations using induced drag polar graph (left) and the  $C_L$  vs AoA graph (right)

These CFD analysis results provide the wing surface load distribution as input for WingSizer

and the aerodynamic coefficients for FAST-OAD. The total load distribution has been calculated by integrating the previously shown pressure and friction stress distributions. For the aerodynamic coefficients, the six components of aerodynamic forces and moments are provided, along with the breakdown of pressure and friction stress, and the values of induced drag.

## 5.2 Wing Structural Analysis and Sizing

For each use case, WingSizer takes as input the loads provided by FaSTAR and the geometrical parameters provided by FAST-OAD's initial iteration, these being the wingspan, tipchord, rootchord, kinkchord, sweep and dihedral. The loads are provided using a set of grids and forces corresponding to a levelled flight load distribution and are multiplied within WingSizer by an ultimate load factor of 1.5 for sizing purposes. While the WingSizer tool allows for an instability calculation of metallic skins, it does not do the same for composite material. Hence, it would not be equitable to compare composite solutions without also considering skin instability. Therefore, for the purposes of the collaborative framework, only static failure scenarios are considered for the comparison between metallic and composite wing components. For metallic components, the tool evaluates the static failure by comparing the resulting von-mises stress ( $f_{vms}$ ) against the material ultimate tensile allowable ( $F_{tu}$ ), as per Equation (1).

$$MS = \frac{F_{tu}}{f_{vms}} - 1 \quad (1)$$

WingSizer increases the components thicknesses and re-runs the updated model until the margin of safety calculated using Equation (1) is positive for all wing components. For composite components, the tool evaluates the static failure of the laminate using the Tsai-Wu failure criteria, as per Equation (2).

$$FI = \left( \frac{1}{X_t} - \frac{1}{X_c} \right) \sigma_1 + \left( \frac{1}{Y_t} - \frac{1}{Y_c} \right) \sigma_2 + \frac{\sigma_1^2}{X_t X_c} + \frac{\sigma_2^2}{Y_t Y_c} + \frac{\sigma_{12}^2}{S^2} + 2F_{12} \sigma_1 \sigma_2 = 1 \quad (2)$$

, where:

- $\sigma_1$  is the ply longitudinal stress
- $\sigma_2$  is the ply transverse stress
- $\sigma_{12}$  is the ply shear stress
- $X_t$  is the tensile stress allowable in the principal x (or 1) direction of the material
- $X_c$  is the compressive stress allowable in the principal x (or 1) direction of the material
- $Y_t$  is the tensile stress allowable in the principal y (or 2) direction of the material
- $Y_c$  is the compressive stress allowable in the principal y (or 2) direction of the material
- $S$  is the shear stress allowable in the principal material system
- $F_{12}$  is the interaction strength constant, experimentally determined

WingSizer increases the number of plies and re-runs the updated model until the respective margin of safety, calculated using Equation (3), becomes positive for all wing components.

$$MS = \frac{1}{F.I.} - 1 \quad (3)$$

The complete WingSizer framework and additional functionalities are explained in detail in Reference [22]. It should be noted that certain **assumptions** are made during the operation of the WingSizer tool. These are as follows:

- The stringers section and material (metallic) remains unchanged regardless of the wing components material choice.

- The model is clamped at the wing root using NASTRAN single point constraints (SPC) with all degrees of freedom restrained. Therefore, the first bay (wing root) components have been disregarded from the analysis due to the existence of unrealistic stress concentration points. Their thickness is set to 4mm for the metallic wings and the number of plies is set to 12 plies for the composite wing to avoid an unrealistic stiffness reduction near the wing root.
- The stringer pitch at the wing root is assumed as 200mm for all use cases. The value of stringer pitch decreases proportionally to the wing chord as one moves from the root to the tip of the wing.
- A rib spacing of approximately 500mm is considered for the baseline case geometry and a spacing of approximately 700mm for the UC1 and UC2 geometry.

The assumed stringer pitch and rib spacing mentioned above are selected based on typical aircraft design values. For the baseline and UC1, Aluminum 2024-T3 has been used within WingSizer as the reference metallic material with the properties presented in Table 4.

Table 4 – Metallic material properties (Al2024-T3, QQ-A-250/4) [25].

Symbol	Value	Units	Description
$E$	72395	MPa	Young's modulus
$\nu$	0.33	–	Poisson coefficient
$\rho$	$2.768 \times 10^{-6}$	kg/mm <sup>3</sup>	Density

For UC2, the composite material properties [26] used within WingSizer are presented in Table 5. The values with an asterisk in Table 5 are not available in the composite material reference and are assumed based on the authors past experience.

Table 5 – Composite material and mechanical properties, Hexply 8552 AGP 280-5H [26]

Symbol	Units	Value	Description
$E_{12}, E_{21}$	MPa	67000, 66000	Elasticity modulus
$G^*$	MPa	5280	Shear modulus
$\nu^*$	-	0.07	Poisson coefficient
$\rho$	kg/mm <sup>3</sup>	$1.57 \times 10^{-6}$	Density
$X_t$	MPa	876	Tensile stress allowable X-direction
$X_c$	MPa	924	Compression stress allowable X-direction
$Y_t$	MPa	800	Tensile stress allowable Y-direction
$Y_c^*$	MPa	844	Compressive stress allowable Y-direction

The final components' thicknesses for the baseline case, UC1 and UC2 are shown in Figure 10, 11 and 12, respectively. The results indicate an increase in mass of 55% when changing the wing configuration from the baseline to the UC1 geometry and a possible wing structural mass saving of approximately 50% when changing all wing components material from metallic to composite i.e. transitioning from UC1 to UC2 geometry. The obtained mass for the baseline configuration is approximately 27% lower than the A320 wing reference mass due to the assumptions considered for the wing sizing. It should be noted that the sized thicknesses presented from Figure 10 to Figure 12 are based on a single levelled flight load case and considering only the two static failure modes assessed using Equations (1) and (2). Additionally, the rib spacing is increased from the baseline to the UC1 geometry.

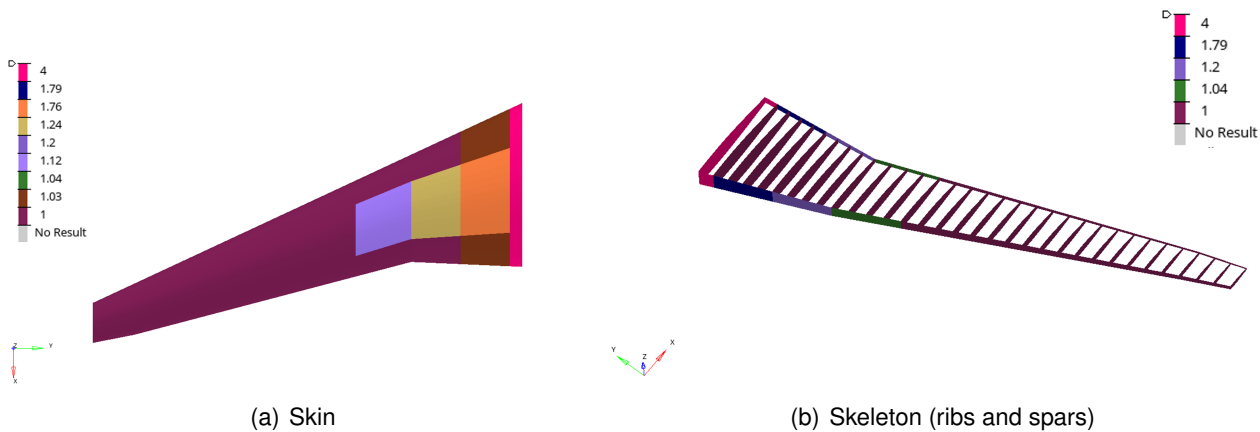


Figure 10 – Baseline Case: Fully metallic components thicknesses [mm].

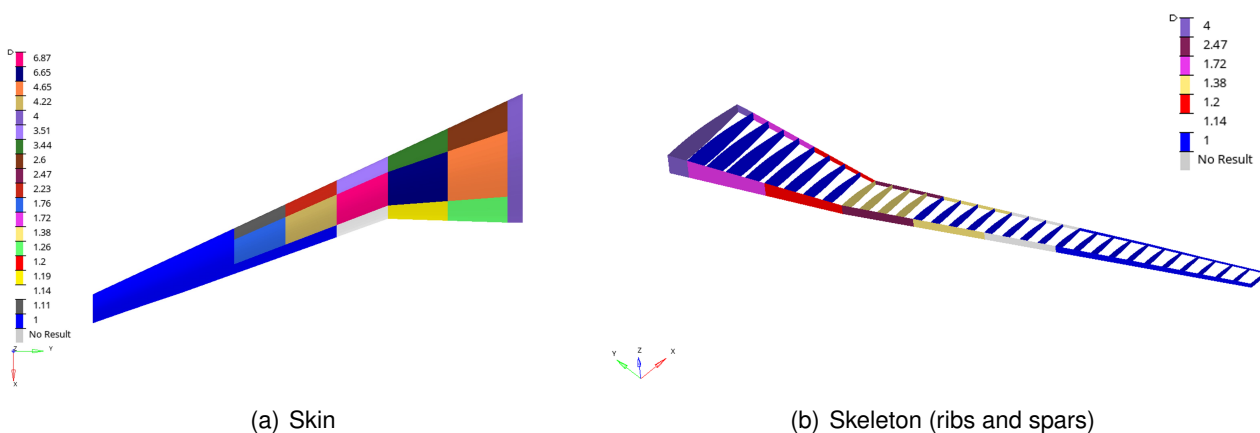


Figure 11 – Use-Case 1: Fully metallic components thicknesses [mm].

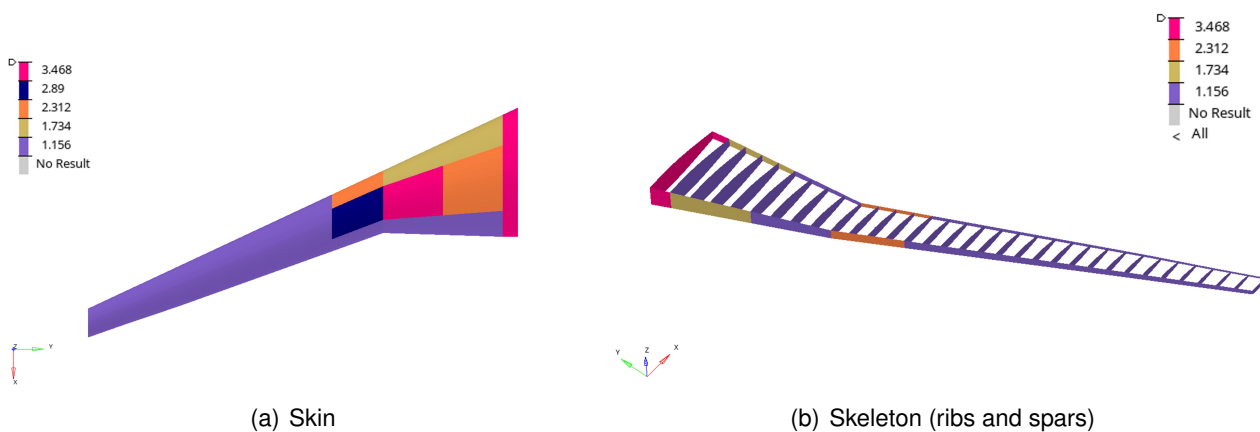


Figure 12 – Use-Case 2: Fully composite components thicknesses [mm].

Once positive margins of safety are achieved for all components, WingSizer outputs the thickness distribution for skins, ribs and spars and the wing structural mass. These outputs, especially the wing structural mass, are then fed back to FAST-OAD to be included in the detailed aircraft mass calculations. The wing structural mass, along with masses from FAST-OAD, serve as an input for DOCpy as well for the direct operating cost calculations.

### 5.3 Overall Aircraft Design and Integration

As previously described in section 3., the OAD process starts with converging an initial feasible aircraft with the help of FAST-OAD. The geometry and weight are then written in the common data exchange file and transmitted to WingSizer and FaSTAR for refined wing structure calculation and CFD analysis, respectively. When the detailed analysis are completed by the partner tools, the new wing weight and aerodynamic performances are used to adjust the tuning coefficients of the OAD process. In more details, the Wingsizer provides weight of the wing primary structure (skin, spars, web, stringers). The difference between the primary structure weight of FAST-OAD and the Wingsizer is used to calculate a new tuning coefficient for the primary structure weight of FAST-OAD. For the aerodynamics, since the focus is high aspect ratio wing, the most important drag term to validate with high fidelity evaluation is the induced drag. This is done by adjusting the Oswald coefficient of FAST-OAD using the induced drag polar determined from the CFD computation. Particularly, between the baseline case and UC1, the high fidelity analysis revealed a 10% higher induced drag than what FAST-OAD predicted. This difference is typical in preliminary design as the OAD process uses simplified aerodynamic performance models that assume ideal lift distribution. This assumption is usually valid but requires a few detailed aerodynamic design iterations, something that is not available at this preliminary design stage. After the new calibration of FAST-OAD is made, a new aircraft is calculated with slightly different geometry and weight that are sent again to the partners for a new high fidelity evaluation and a first DOC calculation. Figure13 shows the baseline wing geometry, visualized in TiGL, as compared to the resultant HAW geometry used for UC1, UC2 and UC3. Some important weight parameters calculated by FAST-OAD are maximum take-off mass, operational empty mass, maximum landing mass, payload mass, fuel mass and engine mass. These are specifically essential for the cost analysis to be performed for each use-case. The process is repeated until convergence is obtained and is identical for all use-cases. For the last use-case with UHBR engine, the BPR is changed from 11 (Leap A1 reference engine) to 16. This change has a direct influence on the fuel efficiency of the aircraft and yielded a 2.5% lower fuel requirement but at a cost of a 9% heavier engine. These masses contribute to the direct operating cost analysis, which is discussed in the following section.

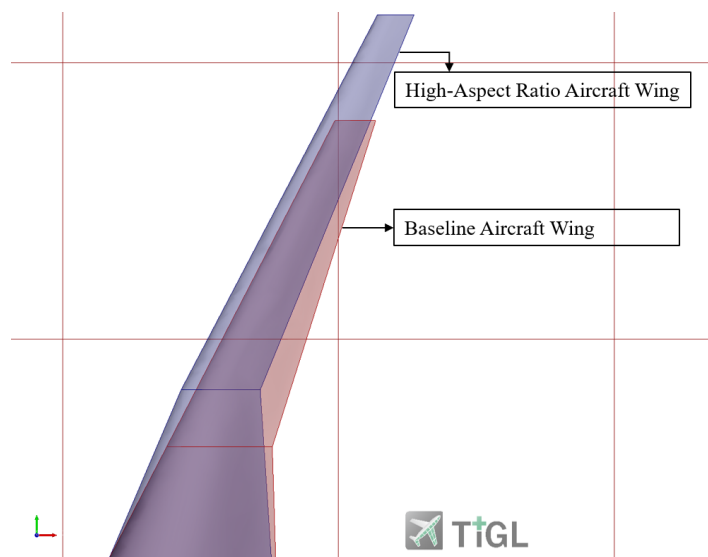


Figure 13 – Wing planform geometries for baseline aircraft configuration and the high aspect ratio wing aircraft configuration, as visualized after importing CPACS xml file, containing wing geometry specifications, into TiGL

### 5.4 Direct Operating Cost Analysis

After the successful execution of FAST-OAD, FaSTAR and WingSizer, a preliminary cost analysis is conducted using DOCpy. For this analysis, the design masses of the aircraft, the cruise velocity and altitude, and engine characteristics are taken into account to roughly estimate costs of operating



the aircraft in an European scenario.

DOCpy receives the fuel mass, operating empty mass and maximum take-off mass from FAST-OAD. In order to adjust the cost estimation according to the material selected for the wing structure, DOCpy also receives the wing mass from WingSizer with an identification whether the material selected is metallic or composites.

In order to compute the operational costs for each case, DOCpy first constructs a payload-range diagram for each use case based on the design masses. In figure 14(a), the results for the baseline case and the 3 use-cases are displayed. The resulting take-off mass is showed on figure 14(b). The dashed line in both graphs indicate the design range selected for the aircraft. Although cases UC1, UC2 and UC3 have the same payload capability, the influences of the wing material and the UHBR engines on take-off mass are significant. The aircraft in cases UC1, UC2, UC3 are operated at the same Mach Number and altitude. Therefore, the masses and the engine will be the main factors influencing costs.

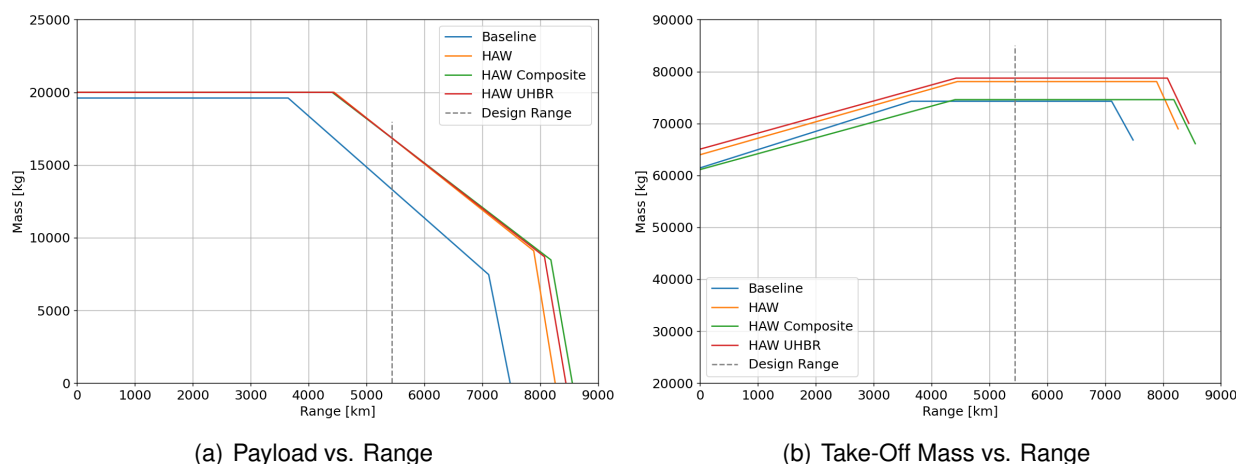


Figure 14 – Comparison of aircraft masses over physical ranges for the different use-cases

In addition to the influence on the design masses, the wing material is assumed to impact the airframe’s capital and maintenance costs by a factor of +2%.

Once the aircraft masses over the range are obtained, DOCpy computes the operating costs and cost per available seat kilometer (CASK) for each case. The results for the latter are shown in Figure 15 for over the aircraft physical range. The total direct operation cost for all aircraft are shown in Table 6. It can be seen that UC2 showed the lowest cost at the design operational range which is largely due to the lower fuel mass requirement and lower wing mass due to the lighter composite material. On the other hand, UC1 and UC3 have very similar values since the effect of UHBR is rather low. Finally, the baseline case is the most costly aircraft to operate, which is expected due to the absence of any of the technological advancements which exist in the other use-cases.

Table 6 – Yearly operating costs in millions of Euros at range equal to 5436 km.

Use Case	DOC [Mill. €]
Baseline	31.58
UC1 - HAW	31.47
UC2 - Composite HAW	30.60
UC3 - HAW + UHBR Engine	31.43

To better understand the cost build-up for each use case, the cost breakdown is shown on figure 16. In terms of capital cost, although an increase in 2% is assigned to the wing of the HAW Composite case, a reduction in capital cost is seen due to an overall reduction in operating empty mass of around

6.5%. The UHBR case presents an increase in capital costs due to the more technological advanced and larger engines.

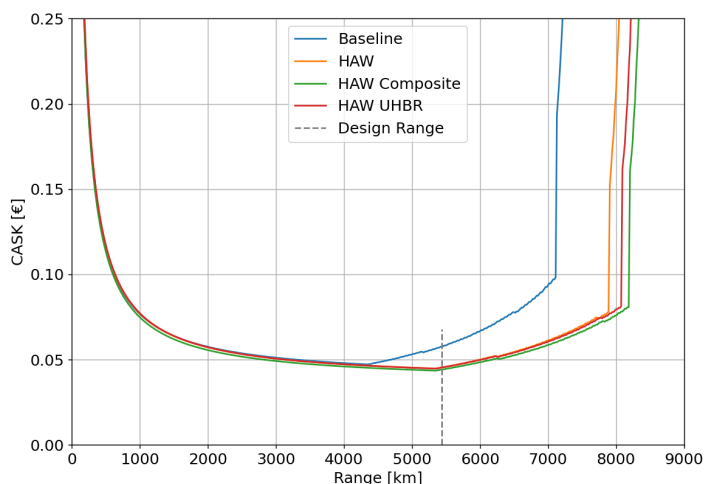


Figure 15 – Comparison of cost per available seat kilometer for each aircraft over their physical ranges.

The lower crew cost for the Baseline aircraft is due to the lower passenger capacity at the required design range, therefore being able to fly with less cabin attendants. The Baseline case also presents lower payload capacity, justifying the difference in the payload handling fees. The maintenance costs have a strong dependence on the airframe and engine weights. A reduction in maintenance costs from UC1 to UC2 can be seen due to the overall reduction in airframe weight, although the composite wing maintenance costs are scaled up by 2%. From the HAW to the HAW with UHBR case, a slight increase in maintenance costs is seen due to the new technology and larger engines.

The biggest differences can be found in the fuel cost. This relates directly to the fuel weights received from FAST-OAD. Lighter and more efficient aircraft require less fuel for flying. Comparing UC1 and UC3 in particular, one can conclude that the improve in fuel consumption due to the UHBR engines offset the increase in costs in the capital, maintenance, landing and ATC fees categories. The landing fees and ATC fees are computed taking the take-off mass as estimation parameter. Therefore, those costs follow the trend in take-off mass seen in figure 14(b).

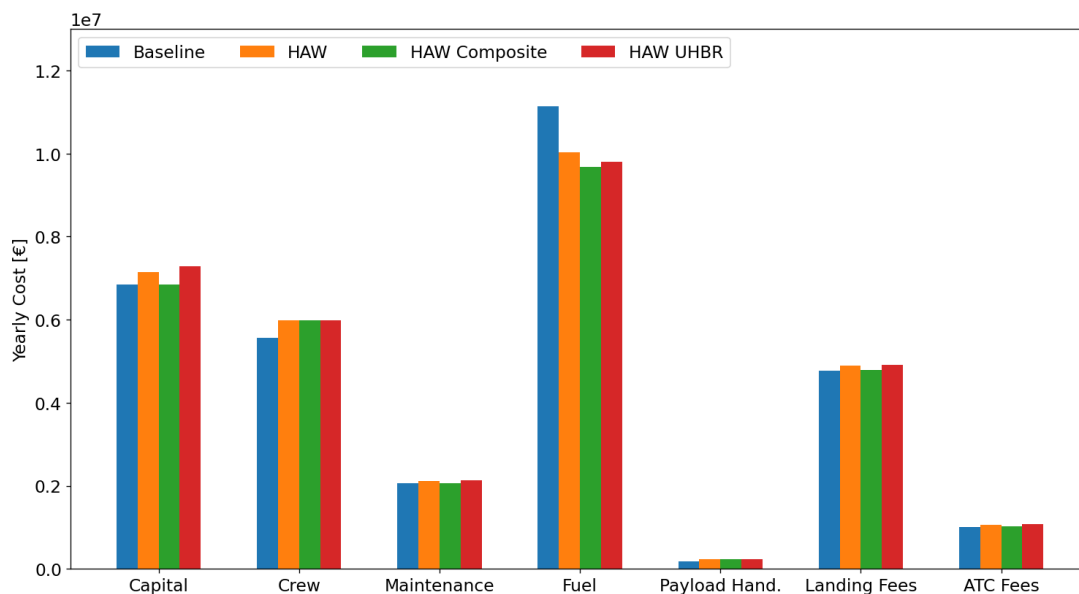


Figure 16 – Breakdown of yearly operational costs for each case investigated.

## 6. Conclusion and Outlook

By the end of the project the aim of introducing the CEF to the next generation of researchers from leading aerospace research organizations of the world, was successfully achieved. The methodology and the framework was validated on two levels. First, on a broader but less detailed level where young engineers from 18 different countries were brought together and trained to adopt the CEF and reap its benefits. Second, on a smaller yet much more detailed level, with the help of a few selected partners, the framework was established to demonstrate its proficiency in being able to tackle complex multi-disciplinary, multi-fidelity and multi-objective problems in a time and resource efficient manner. Three use-cases were analysed to achieve this feat: High aspect ratio wing (HAW) configuration aircraft, HAW aircraft with composite wing structure and HAW aircraft with an Ultra high bypass ratio (UHBR) engine. In order to perform the analysis, four disciplinary tools were chosen: an OAD called FAST-OAD developed by experts at ONERA, a high fidelity CFD tool called FaSTAR by JAXA, a wing structure sizing tool called WingSizer developed by CEiiA and a cost analysis tool by TU Wien.

A reference aircraft design was also finalized for each of the 3 advanced technologies that were investigated. These will serve as a good starting point for future projects which aim to do a more in-depth study into sustainable aircraft design, be it by analysing novel aircraft configurations or by improving the existing ones. Since aircraft design experts from 18 different countries are now acquainted and trained with the CEF, this will not only make future collaborations more probable but also, it will be much easier to collaborate and work together as experts involved will already have experience with the methodology behind effective design processes like using CEF or collaborative MDAO. Another achievement that took place in the course of the IFAR-X project was development of additional competences such as the WingSizer tool by CEiiA[22].

Despite the large number of participants, significant research is still required to address the incomplete and evolving list of disciplinary tools involved in the project. Furthermore, even though CEF is being widely used within some institutes for aircraft design, the fidelity level of the disciplines involved is restricted to low to mid-fidelity tool. The current research made an attempt to include high fidelity tools in the chain for aerodynamics discipline. It is evident that the CEF hold potential to tackle such mixed fidelity workflows, however, it is also clear that more research needs to be made in this direction. Some limitations which were encountered during this project were due to the higher cost of high fidelity analysis tools. This is a well known limitation of such tools, however, when combined with low or mid-fidelity tools in the same workflow, it leads to long waiting times for experts to run their next tool iteration in case of a loop or series workflow execution. Although solutions like using surrogate models or parallel computing techniques exist, these solutions need to be tested out within the CEF.

## 7. Contact Author Email Address

E-mail: Sparsh.Garg@dlr.de

Phone: +49 402 489641329

Address: Hein-Saß-Weg 22, 21129 Hamburg, Germany

## 8. Acknowledgments

The collaboration and the research presented in this paper has been made possible by the efforts made by the IFAR committee and the participating member countries and their experts. The authors would like to acknowledge the effort of DLR (German Aerospace Center) and ONERA (The French Aerospace Lab) members, who organised and hosted the IFAR-ECN 2023 event. The authors would also like to thank André Pereira from CEiiA for contributing with the adjustments necessary for WingG3N to be integrated within WingSizer tool.

## 9. Copyright Statement

The authors confirm that they, and/or their company or organization, hold copyright on all of the original material included in this paper. The authors also confirm that they have obtained permission, from the copyright holder of any third party material included in this paper, to publish it as part of their paper. The authors confirm that

they give permission, or have obtained permission from the copyright holder of this paper, for the publication and distribution of this paper as part of the ICAS proceedings or as individual off-prints from the proceedings.

## References

- [1] Erik Baalbergen, Jos Vankan, Luca Boggero, Jasper H. Bussemaker, Thierry Lefebvre, Bastiaan Beijer, Anne-Liza Bruggeman, and Massimo Mandorino. *Advancing Cross-Organizational Collaboration in Aircraft Development*. American Institute of Aeronautics and Astronautics, Reston, Virginia, 2022.
- [2] Johan Bruneel, Pablo D'Este, and Ammon Salter. Investigating the factors that diminish the barriers to university–industry collaboration. *Research Policy*, 39(7):858–868, 2010.
- [3] Erik Baalbergen, Wim Lammen, Nikita Noskov, Pier-Davide Ciampa, and Erwin Moerland. Integrated collaboration capabilities for competitive aircraft design. *MATEC Web of Conferences*, 233:00015, 2018.
- [4] Thierry Pardessus. Concurrent engineering development and practices for aircraft design at airbus. *24th ICAS Congress*, 2004.
- [5] Erwin Moerland, Pier Davide Ciampa, Sascha Zur, Erik Baalbergen, Nikita Noskov, Roberto D'Ippolito, and Riccardo Lombardi. Collaborative architecture supporting the next generation of mdao within the agile paradigm. *Progress in Aerospace Sciences*, 119:100637, 2020.
- [6] Gary Belie. Non-technical barriers to multidisciplinary optimization in the aerospace industry. 09 2002.
- [7] Pier Davide Ciampa and Björn Nagel. Agile paradigm: The next generation collaborative mdo for the development of aeronautical systems. *Progress in Aerospace Sciences*, 119:100643, 2020.
- [8] Susan X Ying. Report from icas workshop on complex systems integration in aeronautics. 2016.
- [9] Jaroslaw Sobieszczanski-Sobieski, Alan Morris, and Michel Van Tooren. *Multidisciplinary design optimization supported by knowledge based engineering*. John Wiley & Sons, 2015.
- [10] Joaquim R. R. A. Martins and Andrew B. Lambe. Multidisciplinary design optimization: A survey of architectures. *AIAA Journal*, 51(9):2049–2075, 2013.
- [11] Marko Alder, Erwin Moerland, Jonas Jepsen, and Björn Nagel. Recent advances in establishing a common language for aircraft design with cpacs. In *Aerospace Europe Conference*, 2020.
- [12] Andrew B. Lambe and Joaquim R. R. A. Martins. Extensions to the design structure matrix for the description of multidisciplinary design, analysis, and optimization processes. *Structural and Multidisciplinary Optimization*, 46(2):273–284, 2012.
- [13] Andreas Page Risueño, Jasper Bussemaker, Pier Davide Ciampa, and Bjoern Nagel. Mdash: Agile generation of collaborative mdao workflows for complex systems. In *AIAA Aviation 2020 Forum*, page 3133, 2020.
- [14] Brigitte Boden, Jan Flink, Niklas Först, Robert Mischke, Kathrin Schaffert, Alexander Weinert, Annika Wohlan, and Andreas Schreiber. Rce: An integration environment for engineering and science. *SoftwareX*, 15:100759, 2021.
- [15] Brigitte Boden, Jan Flink, Robert Mischke, Kathrin Schaffert, Alexander Weinert, Annika Wohlan, and Andreas Schreiber. *RCE*. Zenodo, 2019.
- [16] Martin Siggel, Jan Kleinert, Tobias Stollenwerk, and Reinhold Maierl. Tigl: An open source computational geometry library for parametric aircraft design. *Mathematics in Computer Science*, 13, 09 2019.
- [17] Yiyuan Ma and Ali Elham. Designing high aspect ratio wings: A review of concepts and approaches. *Progress in Aerospace Sciences*, 145, 02 2024.
- [18] Graeme Kennedy and Joaquim Martins. A comparison of metallic and composite aircraft wings using aerostructural design optimization. 09 2012.
- [19] S Ebadi, K Shahbazi, and E Anbarzadeh. Investigation of aluminum and composite aircraft wings under the influence of aerodynamic forces and their effects on environmental impacts. *Journal of Environmental Friendly Materials*, 5(1):13–21, 2021.
- [20] Daniel Giesecke, Marcel Lehmler, Jens Friedrichs, Jason Blinstrub, Lothar Bertsch, and Wolfgang Heinze. Evaluation of ultra-high bypass ratio engines for an over-wing aircraft configuration. 2:493–515.
- [21] Christophe David, Scott Delbecq, Sebastien Defoort, Peter Schmollgruber, Emmanuel Benard, and Valerie Pommier-Budinger. From fast to fast-oad: An open source framework for rapid overall aircraft design. *IOP Conference Series Materials Science and Engineering*, 1024:012062, 01 2021.
- [22] Pedro F. Albuquerque, Ana M. P. Silva, and André N. Pereira. Aircraft wing structural sizing computational tool tailored for a collaborative multidisciplinary design framework. *34th ICAS Congress*, inproceedings 2024.
- [23] Atsushi Hashimoto, Keiichi Murakami, Takashi Aoyama, Keiichi Ishiko, Manabu Hishida, Masahide

Sakashita, and Paulus Lahur. Toward the fastest unstructured cfd code "fastar". *50th AIAA Aerospace Sciences Meeting Including the New Horizons Forum and Aerospace Exposition*, 01 2012.

[24] EUROCONTROL CRCO. Customer guide to charges, 2022.

[25] Federal Aviation Administration. Metallic materials properties development and standardization (mmpds). 2010.

[26] Hexcel properties datasheet - hexply 8552 epoxy matrix (180°c curing matrix).